Reduction Potential Tuning of the Blue Copper Center in Pseudomonas aeruginosa Azurin by the Axial Methionine as Probed by Unnatural Amino Acids

7 AUTHORS, INCLUDING:

Mark Vaughan
Quest University Canada
11 PUBLICATIONS 498 CITATIONS

SEE PROFILE

Masha Savelieff
University of Michigan
25 PUBLICATIONS 880 CITATIONS

SEE PROFILE

John F Honek
University of Waterloo
106 PUBLICATIONS 1,898 CITATIONS

SEE PROFILE

Yi Lu
Nanjing University
399 PUBLICATIONS 14,474 CITATIONS

SEE PROFILE

Reduction Potential Tuning of the Blue Copper Center in *Pseudomonas aeruginosa* Azurin by the Axial Methionine as Probed by Unnatural Amino Acids

Dewain K. Garner,[†] Mark D. Vaughan,[‡] Hee Jung Hwang,[†] Masha G. Savelieff,[†] Steven M. Berry,[†] John F. Honek,*,[‡] and Yi Lu*,[†]

Contribution from the Department of Chemistry, University of Illinois at Urbana-Champaign, Urbana, Illinois 61801 and the Department of Chemistry, University of Waterloo, Waterloo, Ontario, Canada N2L 3G1

Received April 19, 2006; E-mail: yi-lu@uiuc.edu; jhonek@uwaterloo.ca

Abstract: The conserved axial ligand methionine 121 from *Pseudomonas aeruginosa* azurin (Az) has been replaced by isostructural unnatural amino acid analogues, oxomethionine (OxM), difluoromethionine (DFM), trifluoromethionine (TFM), selenomethionine (SeM), and norleucine (Nle) using expressed protein ligation. The replacements resulted in <6 nm shifts in the S(Cys)−Cu charge transfer (CT) band in the electronic absorption spectra and <8 gauss changes in the copper hyperfine coupling constants ($A_{||}$) in the X-band electron paramagnetic resonance spectra, suggesting that isostructural replacement of Met resulted in minimal structural perturbation of the copper center. The slight blue shifts of the CT band follow the trend of stronger electronegativity of the ligands. This trend is supported by ^{19}F NMR studies of the fluorinated methionine analogues. However, the order of $A_{||}$ differs, suggesting additional factors influencing $A_{||}$. In contrast to the small changes in the UV−vis and EPR spectra, a large variation of >227 mV in reduction potential was observed for the series of variants reported here. Additionally, a linear correlation was established between the reduction potentials and hydrophobicity of the variants. Extension of this analysis to other type 1 copper-containing proteins reveals a linear correlation between change in hydrophobicity and change in reduction potential, independent of the protein scaffold, experimental conditions, measurement techniques, and steric modifications. This analysis has also revealed for the first time high and low potential states for type 1 centers, and the difference may be attributable to destabilization of the protein fold by disruption of hydrophobic or hydrogen bonding interactions that stabilize the type 1 center.

Introduction

Azurin (Az) is a blue, or type 1, copper protein involved in electron transfer.[1−8] The copper center is characterized by an intense blue color arising from a ligand to metal charge transfer (LMCT) band near 625 nm ($\epsilon \approx 5000\ M^{-1}\ cm^{-1}$). Narrow copper hyperfine coupling constants ($A_{||} \sim 60$ G) are also characteristic of this family of proteins. The copper coordination sphere is nearly trigonal bipyramidal and consists of two histidines (His46 and His117) and one Cys112 in the equatorial positions with weaker interactions with Met121 and a backbone carbonyl (Gly45) in the axial positions to the copper (Figure 1). The copper cysteine bond is unusually short (∼2.1 Å) and,

[†] University of Illinois at Urbana-Champaign.

[‡] University of Waterloo.

(1) Gray, H. B.; Malmström, B. G.; Williams, R. J. P. *J. Biol. Inorg. Chem.* **2000**, *5*, 551−559.

(2) Solomon, E. I.; Randall, D. W.; Glaser, T. *Coord. Chem. Rev.* **2000**, *200−202*, 595−632.

(3) Vila, A. J.; Fernández, C. O. In *Handbook on Metalloproteins*; Bertini, I.; Sigel, A.; Sigel, H., Eds.; Marcel Dekker: New York, 2001, pp 813−856.

(4) Lu, Y. In *Comprehensive Coordination Chemistry II: From Biology to Nanotechnology*; McCleverty, J., Meyer, T. J., Eds.; Vol. 8 (*Biocoordination Chemistry*; Que, L., Jr., Tolman, W. B., Eds.); Elsevier: 2004; pp 91−122. Eds. Elsevier: Oxford, UK, 2004; pp 91−122.

(5) Solomon, E. I.; Szilagyi, R. K.; DeBeer George, S.; Basumallick, L. *Chem. Rev. (Washington, DC)* **2004**, *104*, 419−458.

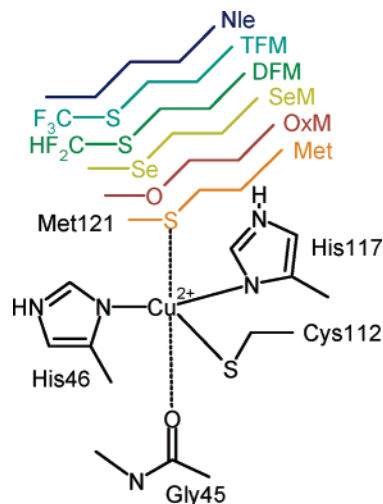(6) Dennison, C. *Coord. Chem. Rev.* **2005**, *249*, 3025−3054.

Figure 1. The blue copper center in Az, showing isostructural replacement of the conserved axial ligand methionine (Met121) with unnatural amino acids oxomethionine (OxM), selenomethionine (SeM), difluoromethionine (DFM), trifluoromethionine (TFM), or norleucine (Nle).

on the basis of experimental and computational findings, is highly covalent.[7] It is this bond that generates the intense charge-transfer band characteristic of blue copper centers.[2]

All type 1 copper proteins display reduction potentials higher than that of aqueous copper ions. Consequently, much work has been directed at elucidating the characteristics of the protein environment that control the copper ion's reduction potential. Desolvation of the copper ion, protein restriction of metal coordination geometry (rack mechanism), metal ligand interactions, intraprotein charge interactions, and hydrogen bonding to metal ligands (particularly S_{Cys}) have all been proposed to affect the reduction potential (reference 1−8 and references therein).

Of particular interest are the effects exerted by the axial Met and backbone carbonyl. At a distance of ∼3 Å, as reported in the initial crystal structure of Az,[9] little covalent interaction between the copper and backbone carbonyl is expected.[2,10] However, higher resolution crystal structures place this bond length significantly closer, at 2.6 Å,[11] suggesting that this axial interaction may be important. This conclusion has also been supported by computational studies.[8,12] The copper thioether bond (∼2.8 Å) to methionine has also drawn considerable attention.[5,13] Some type 1 copper centers, such as stellacyanin and fungal laccase, naturally lack the axial methionine and have other residues such as Gln or Phe at the axial position. Consequently, the axial methionine in Az has been mutated to almost every other natural amino acid[14−19] in an effort to elucidate the exact role played by this residue in controlling the copper redox couple. Some variants have even allowed binding of small exogenous ligands at the axial position.[20−22] Other studies have mutated the axial ligand of type 1 centers in other proteins such as nitrite reductase,[23−25] amicyanin,[26] rusticyanin,[27] pseudoazurin,[28] laccase,[29] and stellacyanin.[30−33]

These studies have pointed out a number of roles the axial ligand can play in the blue copper center, including steric protection of the copper ion from interaction with water and exogenous ligands,[16,20,22,34−36] electronic modulation of the "in-plane" S(Cys)−Cu(II) interaction,[14,37−39] control of the geometry of the blue copper center,[38,40−44] and fine-tuning of the stability of the oxidation states of the copper ion[13,45] and thus the reduction potential of the blue copper site.[26,34,46,47]

Despite the tremendous progress made in studying blue copper proteins and their axial ligand variants, the precise role of the axial Met in modulating the blue copper center is still uncertain, and correlation of the structural properties of the axial ligand with copper reduction potentials is difficult to obtain. Due to the limitation of only 20 natural amino acids, site-directed mutagenesis has not been able to accurately distinguish between multiple variances introduced by the same mutation. For example, a single mutation may alter, to different degrees, numerous parameters such as geometry, sterics, electronic interactions, solvent exposure, and hydrophobicity. We previously reported replacement of the Az axial methionine with its unnatural amino acid isostructural analogues selenomethionine (SeM) and norleucine (Nle).[48] This approach allows one to probe the effect of only one or two factors of the axial ligand, such as hydrophobicity, while eliminating or minimizing other parameters such as steric and geometric parameters and solvent exposure. Incorporation of the unnatural amino acids was accomplished using the express protein ligation (EPL) method[49] that couples a bacterially expressed N-terminal protein to a synthetic C-terminal peptide containing the unnatural amino

(7) Shadle, S. E.; Penner-Hahn, J. E.; Schugar, H. J.; Hedman, B.; Hodgson, K. O.; Solomon, E. I. *J. Am. Chem. Soc.* **1993**, *115*, 767−776.
(8) Li, H.; Webb, S. P.; Ivanic, J.; Jensen, J. H. *J. Am. Chem. Soc.* **2004**, *126*, 8010−8019.
(9) Nar, H.; Messerschmidt, A.; Huber, R.; van der Kamp, M.; Canters, G. W. *J. Mol. Biol.* **1991**, *221*, 765−772.
(10) Lowery, M. D.; Solomon, E. I. *Inorg. Chim. Acta* **1992**, *198−200*, 233−243.
(11) Crane, B. R.; Di Bilio, A. J.; Winkler, J. R.; Gray, H. B. *J. Am. Chem. Soc.* **2001**, *123*, 11623−11631.
(12) Olsson, M. H. M.; Ryde, U. *J. Biol. Inorg. Chem.* **1999**, *4*, 654−663.
(13) Solomon, E. I.; Penfield, K. W.; Gewirth, A. A.; Lowery, M. D.; Shadle, S. E.; Guckert, J. A.; LaCroix, L. B. *Inorg. Chim. Acta* **1996**, *243*, 67−78.
(14) Karlsson, B. G.; Nordling, M.; Pascher, T.; Tsai, L.-C.; Sjolin, L.; Lundberg, L. G. *Protein Eng.* **1991**, *4*, 343−349.
(15) Pascher, T.; Karlsson, B. G.; Nordling, M.; Malmström, B. G.; Vänngård, T. *Eur. J. Biochem.* **1993**, *212*, 289−296.
(16) Kroes, S. J.; Hoitink, C. W. G.; Andrew, C. R.; Ai, J.; Sanders-Loehr, J.; Messerschmidt, A.; Hagen, W. R.; Canters, G. W. *Eur. J. Biochem.* **1996**, *240*, 342−351.
(17) Murphy, L. M.; Strange, R. W.; Karlsson, B. G.; Lundberg, L. G.; Pascher, T.; Reinhammar, B.; Hasnain, S. S. *Biochemistry* **1993**, *32*, 1965−1975.
(18) Karlsson, B. G.; Aasa, R.; Malmström, B. G.; Lundberg, L. G. *FEBS Lett.* **1989**, *253*, 99−102.
(19) Di Bilio, A. J.; Chang, T. K.; Malmström, B. G.; Gray, H. B.; Karlsson, B. G.; Nordling, M.; Pascher, T.; Lundberg, L. G. *Inorg. Chim. Acta* **1992**, *198−200*, 145−148.
(20) Bonander, N.; Karlsson, B. G.; Vänngård, T. *Biochemistry* **1996**, *35*, 2429−2436.
(21) Vidakovic, M.; Germanas, J. P. *Angew. Chem., Int. Ed.* **1995**, *34*, 1622−1624.
(22) Tsai, L.-C.; Bonander, N.; Harata, K.; Karlsson, G.; Vänngård, T.; Langer, V.; Sjölin, L. *Acta Crystallogr. Sect. D: Biol. Crystallogr.* **1996**, *D52*, 950−958.
(23) Olesen, K.; Veselov, A.; Zhao, Y.; Wang, Y.; Danner, B.; Scholes, C. P.; Shapleigh, J. P. *Biochemistry* **1998**, *37*, 6086−6094.
(24) Kataoka, K.; Yamaguchi, K.; Sakai, S.; Takagi, K.; Suzuki, S. *Biochem. Biophys. Res. Commun.* **2003**, *303*, 519−524.
(25) Hough, M. A.; Ellis, M. J.; Antonyuk, S.; Strange, R. W.; Sawers, G.; Eady, R. R.; Hasnain, S. S. *J. Mol. Biol.* **2005**, *350*, 300−309.
(26) Diederix, R. E. M.; Canters, G. W.; Dennison, C. *Biochemistry* **2000**, *39*, 9551−9560.
(27) Hall, J. F.; Kanbi, L. D.; Strange, R. W.; Hasnain, S. S. *Biochemistry* **1999**, *38*, 12675−12680.
(28) Kataoka, K.; Kondo, A.; Yamaguchi, K.; Suzuki, S. *J. Inorg. Biochem.* **2000**, *82*, 79−84.
(29) Xu, F.; Palmer, A. E.; Yaver, D. S.; Berka, R. M.; Gambetta, G. A.; Brown, S. H.; Solomon, E. I. *J. Biol. Chem.* **1999**, *274*, 12372−12375.
(30) Nersissian, A. M.; Immoos, C.; Hill, M. G.; Hart, P. J.; Williams, G.; Herrmann, R. G.; Valentine, J. S. *Protein Sci.* **1998**, *7*, 1915−1929.
(31) DeBeer George, S.; Basumallick, L.; Szilagyi, R. K.; Randall, D. W.; Hill, M. G.; Nersissian, A. M.; Valentine, J. S.; Hedman, B.; Hodgson, K. O.; Solomon, E. I. *J. Am. Chem. Soc.* **2003**, *125*, 11314−11328.
(32) Kataoka, K.; Nakai, M.; Yamaguchi, K.; Suzuki, S. *J. Inorg. Biochem.* **1999**, *74*, 188.
(33) Harrison, M. D.; Dennison, C. *ChemBioChem* **2004**, *5*, 1579−1581.
(34) Farver, O.; Skov, L. K.; Pascher, T.; Karlsson, B. G.; Nordling, M.; Lundberg, L. G.; Vänngård, T.; Pecht, I. *Biochemistry* **1993**, *32*, 7317−7322.
(35) Bauer, R.; Danielsen, E.; Hemmingsen, L.; Bjerrum, M. J.; Hansson, O.; Singh, K. *J. Am. Chem. Soc.* **1997**, *119*, 157−162.
(36) Salgado, J.; Kroes, S. J.; Berg, A.; Moratal, J. M.; Canters, G. W. *J. Biol. Chem.* **1998**, *273*, 177−185.
(37) Palmer, A. E.; Randall, D. W.; Xu, F.; Solomon, E. I. *J. Am. Chem. Soc.* **1999**, *121*, 7138−7149.
(38) DeBeer, S.; Randall, D. W.; Nersissian, A. M.; Valentine, J. S.; Hedman, B.; Hodgson, K. O.; Solomon, E. I. *J. Phys. Chem. B* **2000**, *104*, 10814−10819.
(39) Randall, D. W.; George, S. D.; Holland, P. L.; Hedman, B.; Hodgson, K. O.; Tolman, W. B.; Solomon, E. I. *J. Am. Chem. Soc.* **2000**, *122*, 11632−11648.
(40) Lu, Y.; LaCroix, L. B.; Lowery, M. D.; Solomon, E. I.; Bender, C. J.; Peisach, J.; Roe, J. A.; Gralla, E. B.; Valentine, J. S. *J. Am. Chem. Soc.* **1993**, *115*, 5907−5918.
(41) Han, J.; Loehr, T. M.; Lu, Y.; Valentine, J. S.; Averill, B. A.; Sanders-Loehr, J. *J. Am. Chem. Soc.* **1993**, *115*, 4256−4263.
(42) LaCroix, L. B.; Shadle, S. E.; Wang, Y.; Averill, B. A.; Hedman, B.; Hodgson, K. O.; Solomon, E. I. *J. Am. Chem. Soc.* **1996**, *118*, 7755−7768.
(43) Messerschmidt, A.; Prade, L.; Kroes, S. J.; Sanders-Loehr, J.; Huber, R.; Canters, G. W. *Proc. Natl. Acad. Sci. U.S.A.* **1998**, *95*, 3443−3448.
(44) LaCroix, L. B.; Randall, D. W.; Nersissian, A. M.; Hoitink, C. W. G.; Canters, G. W.; Valentine, J. S.; Solomon, E. I. *J. Am. Chem. Soc.* **1998**, *120*, 9621−9631.
(45) Frank, P.; Licht, A.; Tullius, T. D.; Hodgson, K. O.; Pecht, I. *J. Biol. Chem.* **1985**, *260*, 5518−5525.
(46) Romero, A.; Hoitink, C. W. G.; Nar, H.; Huber, R.; Messerschmidt, A.; Canters, G. W. *J. Mol. Biol.* **1993**, *229*, 1007−1021.
(47) Malmström, B. G.; Wittung-Stafshede, P. *Coord. Chem. Rev.* **1999**, *185−186*, 127−140.
(48) Berry, S. M.; Ralle, M.; Low, D. W.; Blackburn, N. J.; Lu, Y. *J. Am. Chem. Soc.* **2003**, *125*, 8760−8768.
(49) Severinov, K.; Muir, T. W. *J. Biol. Chem.* **1998**, *273*, 16205−16209.

acids at the axial ligand position. This method resulted in a high yield of proteins for biophysical characterization. Studies of the Az variants containing the unnatural amino acids suggested a linear correlation of the reduction potential with the hydrophobicity of the axial ligand side chain.[48] However, replacing Met with only two unnatural amino acids (SeM and Nle) and clustering of the points at either end of the hydrophobicity scale in the plot left questions as to the generality of such a correlation.

Herein, we report the expansion of the Az variant series with isostructural methionine replacements. In addition to thioether (Met), selenoether (SeM), and alkyl carbon (Nle) groups, methyl fluorinated thioethers, both difluoro (DFM) and trifluoro (TFM), and an ether (OxM) group were incorporated as methionine isostructural analogues (Figure 1). These additional axial substitutions have demonstrated unambiguously the linear correlation between hydrophobicity of the axial ligand and the reduction potential in type 1 copper centers. Armed with this information, we also examined the correlation of all reported reduction potentials of blue copper centers with their axial ligand variants, and our findings firmly establish hydrophobicity as the dominant factor in reduction potential tuning by the axial ligand, independent of the protein scaffold, experimental conditions, measurement techniques, and steric modifications. More importantly, we discovered high and low potential states for the type 1 centers, and the structural features that may be responsible for such differences are discussed.

Experimental Methods

Materials Including Synthesis of Unnatural Amino Acids. Chemicals purchased from commercial sources were of analytical grade or higher purity. Fmoc-O-methylhomoserine (OxM) was purchased from Senn Chemicals. The L-forms of DFM and TFM were synthetically prepared as previously described.[50−52] Met analogues were protected as the 9-fluorenylmethoxycarbonyl (Fmoc) derivatives according to the method of Paquet.[53] To a stirred solution of sodium bicarbonate (45 mg, 0.53 mmol) in 10 mL 1:1 H_2O/acetone was added either DFM (100 mg, 0.54 mmol) or TFM (109 mg, 0.54 mmol) and N-(9-fluorenylmethoxycarbonyloxy)succinimide (181 mg, 0.54 mmol). The resulting mixture was stirred overnight and then acidified to pH 2 with concd HCl. The acetone was removed *in vacuo*, and the aqueous layer was extracted with 3×1 mL chloroform. The pooled organic extracts were washed with water until neutral, dried over anhydrous sodium sulfate, and evaporated to give a light yellow oil. Recrystallization from CH_2Cl_2/hexanes afforded a white solid. Fmoc-DFM yield was 199 mg (96%). R_f (EtOAc/hexanes) 0.49; mp 129−130 °C; ^{1}H NMR (300 MHz, CDCl₃) δ (relative to tetramethylsilane, 0.00 ppm) 10.65 (s, 1H, CO₂H), 7.75 (2H), 7.56 (2H), 7.39 (2H), 7.32 (2H), 6.79 (t, 1H, CHF₂, J_{HF} = 54.2 Hz), 5.26 (1H, CONH), 4.58 (m, 1H, fluorene C₉H), 4.43 (m, 2H, COCH_2), 4.20 (t, 1H, C$_\alpha H$, J = 7.0 Hz), 2.83 (m, 2H, C$_\gamma$H₂), 2.29 (m, 1H, C$_\beta$H$_A$), 2.04 (m, 1H, C$_\beta$H$_B$); ^{13}C NMR (75.5 MHz, CDCl₃) δ 176.3 (*C*O₂H), 156.8 (O*C*ONH), 147.8 (fluorene C_{10}, C_{11}), 141.4 (fluorene C_{12}, C_{13}), 127.9 (fluorene C_3, C_6), 127.2 (fluorene C_2, C_7), 125.1 (fluorene C_1, C_8), 120.5 (*C*HF₂, J_{CF} = 271.8 Hz), 120.1 (fluorene C_4, C_5), 67.2 (O*C*H₂), 52.8 (*C*$_\alpha$), 47.2 (fluorene C_9), 26.1 (*C*$_\beta$), 23.5 (*C*$_\gamma$); ^{19}F NMR (282.3 MHz, CDCl₃) −93.02 (dd, J_{FF} = 242.6 Hz); HRMS (ESI) calculated for $C_{20}H_{19}NO_4F_2S$ 407.4312, observed 408.4305 (M + H⁺). Fmoc-TFM yield was 208 mg (94%). R_f (EtOAc/hexanes)

0.54; mp 138−139 °C; ^{1}H NMR (300 MHz, CDCl₃) δ (relative to tetramethylsilane, 0.00 ppm) 10.67 (s, 1H, CO₂H), 7.73 (2H), 7.59 (2H), 7.41 (2H) 7.35 (2H), 5.26 (1H, CONH), 4.67 (m, 1H fluorene C₉H), 4.42 (m, 2H, COCH_2), 4.24 (t, 1H, C$_\alpha H$, J = 7.0 Hz), 2.85 (m, 2H, C$_\gamma$H₂), 2.32 (m, 1H, C$_\beta$H$_A$), 2.01 (m, 1H, C$_\beta$H$_B$); ^{13}C NMR (75.5 MHz, DMSO) δ 173.2 (*C*O₂H), 157.3 (O*C*ONH), 148.1 (fluorene C_{10}, C_{11}), 141.3 (fluorene C_{12}, C_{13}), 127.4 (fluorene C_3, C_6), 126.8 (fluorene C_2, C_7), 126.4 (*C*F₃, J_{CF} = 322.84 Hz) 125.3 (fluorene C_1, C_8), 119.6 (fluorene C_4, C_5), 67.3 (O*C*H₂), 53.0 (*C*$_\alpha$), 26.0 (*C*$_\beta$), 24.9 (*C*$_\gamma$) [Note: fluorene C_9 signal obscured by DMSO (47.7 ppm)]; HRMS (ESI) calculated for $C_{20}H_{18}NO_4F_3S$ 425.4201, observed 426.4210 (M + H⁺).

Peptide Synthesis. The synthetic peptide sequences H₂N-CysThrPheGlyHisSerAlaLeu(Met, Nle, SeM, DFM, TFM, or OxM)-LysGlyThrLeuThrLeuLys-COOH were synthesized using optimized Fmoc procedures[54] in N,N-dimethylformamide (DMF) on Fmoc-Lys-(Boc)-Wang resin using a Model 90 peptide synthesizer from Advanced Chem Tech. Deprotection was accomplished by 20% (v/v) piperidine in DMF, and activation of the amino acids was accomplished by ∼4 equiv of 2-(1H-benzotriazole-1-yl)-1,1,3,3-tetramethyluronium hexafluorophosphate (HBTU) in DMF. Due to limited availability, fluoromethionine analogue coupling used only 1 equiv of the Met analogue in conjunction with 1.5 equiv of the activator 2-(7-aza-1H-benzotriazole-1-yl)-1,1,3,3-tetramethyluronium hexafluorophosphate (HATU). Resin and protected natural amino acids were purchased from Chem Impex International (Wood Dale, IL). Protecting groups used were Fmoc-Ala-OH, Fmoc-Asn(trt)-OH, Fmoc-Cys(StBu)-OH, Fmoc-Glu(OtBu)-OH, Fmoc-Gly-OH, Fmoc-His(Boc)-OH, Fmoc-Ile-OH, Fmoc-Leu-OH, Fmoc-Lys(Boc)-OH, Fmoc-Met-OH, Fmoc-Phe-OH, Fmoc-Pro-OH, Fmoc-Ser(tBu)-OH, and Fmoc-Thr(tBu)OH. Following peptide assembly, the full length peptide was cleaved from the beads by treatment with 10 mL trifluoroacetic acid with 0.5 mL each of water, thioanisole, and anisole as scavengers. The cleavage solution was removed under reduced pressure, and the peptide was precipitated by addition of cold diethyl ether. The crude peptide was purified by HPLC using a Waters Delta 600 instrument with a 130 mm × 25 mm C18 preparative column in a Waters PrepLC 25 mm Module. Elution was accomplished with (A) 0.1% TFA in water and (B) 0.08% TFA in 20% water, 80% acetonitrile by a gradient from 20 to 50% B over 45 min. Fractions containing the desired peptide were pooled, lyophilized, and examined by MALDI-TOF mass spectrometry.

Intein Expression and Ligation Conditions. For M121SeM Az, M121Nle Az, M121OxM Az, and M121DFM Az variants, the first 111 amino acids of Az were expressed connected to an intein and chitin binding domain and subsequently isolated and reacted with the corresponding synthetic peptide as previously described.[48] Modifications to the procedure for the isolation and purification of the fusion protein were made for M121TFM Az to improve yield and purity. For this variant, expression was effected using the pTXB1 vector (New England Biolabs, Ipswich, MA), in BLR(DE3) *E. coli* (Novagen, Madison, WI) grown in 2L LB medium at 30 °C for 12 h without induction. After cell lysis by a French pressure cell in 20 mM TrisHCl pH 8.0 (containing 500 mM NaCl, 1 mM EDTA, 1 mM PMSF, 0.1% Triton X-100), the lysate was clarified by centrifugation without attempting to solubilize any existing inclusion bodies. Chitin beads (12 mL; New England Biolabs, Ipswich, MA) previously equilibrated in 20 mM TrisHCl pH 8.0, 500 mM NaCl were subsequently added to the clarified lysate and shaken gently at 4 °C for 1 h. Following removal of the supernatant, the chitin beads were loaded into two 6 mL columns and washed with five column volumes of 20 mM TrisHCl pH 8.0, 500 mM NaCl. Reactions were initiated by the addition of 4 mL of cleavage buffer containing 20 mM TrisHCl pH 8.0, 500 mM NaCl, 1 mM EDTA, 50 mM N-mercaptoacetamide (NMA), and 10 mg of synthetic peptide to each column. Reactions were allowed to proceed for 60 h at 4 °C with gentle shaking. After reaction, the proteins were eluted from the

(50) Houston, M. E.; Honek, J. F. *J. Chem. Soc., Chem. Commun.* **1989**, 761−762.
(51) Houston, M.; Harvath, L.; Honek, J. F. *Bioorg. Med. Chem. Lett.* **1997**, 7, 3007−3012.
(52) Vaughan, M. D.; Cleve, P.; Robinson, V.; Duewel, H. S.; Honek, J. F. *J. Am. Chem. Soc.* **1999**, 121, 8475−8478.
(53) Paquet, A. *Can. J. Chem.* **1982**, 60, 976−980.

(54) Wellings, D. A.; Atherton, E. *Methods Enzymol.* **1997**, 289, 44−67.

column and exchanged into 50 mM ammonium acetate pH 5.1. Copper incorporation was achieved by the incremental addition of 10 mM $CuSO_4$ until saturation was measured at 625 nm. The protein was then further purified on a POROS 20 HQ resin column with an AKTA basic HPLC system (GE Healthcare, Piscataway, NJ).

Electrochemical Measurements. Reduction potentials were obtained using 2 mm^2 pyrolytic graphite edge (PGE) electrodes assembled according to literature procedures.[55] After the electrode surface was polished, 1 μL of protein solution ($\sim$0.1 mM) was applied to the electrode. Following a short incubation (<3 min), the electrode was immersed in 20 mM NH_4OAc pH 4.0, 100 mM NaCl on ice. The potential of the working electrode was varied at a rate of 0.5 V/s with a CH Instruments model 620A Electrochemical Analyzer potentiostat. Although some scan rate dependence of the observed reduction potential has been reported for these conditions,[55] the increased signal obtained at this elevated scan rate makes determination of the reduction potential more certain. We have evaluated the scan rate dependence of the reduction potential of wild type Az at 0.5 and 0.1 V/s from both oxidative and reductive posies and find the value to vary by no more than 10 mV (data not shown). All reduction potentials were measured against Ag/AgCl and converted to normal hydrogen electrode (NHE) potentials by calibration of the silver electrode against a standard calomel electrode (SCE).

Spectroscopic Characterization. UV—visible absorption spectra were obtained on a Varian Cary 3E spectrophotometer at 10 °C. X-band EPR spectra were collected with a Varian 122 spectrometer equipped with an Air Products Helitran cryostat maintained by the University of Illinois NIH EPR Research Center. Samples were analyzed as a frozen glass between 17 and 30 K. Simulation of the EPR spectra was performed using SIMPOW6[56,57] to determine g and $A_\parallel$ values.

^{19}F NMR data (564.5 MHz) were collected utilizing a Bruker Avance 600 MHz NMR spectrometer fitted with a 5 mm dual ^{19}F/^{1}H probehead tuned to ^{19}F. Spectra were recorded at 278 K and referenced to an external sample of a solution of 0.05% trifluorotoluene in CDCl$_3$ (set at -63 ppm) as an external reference. Deprotected TFM-containing peptide (1.5 mg) was dissolved in a 1:1 solution of CD$_3$CN:D$_2$O (total volume of 500 μL). Standard parameters were 30 864 Hz sweep width, 1.06 s acquisition time, and a 1.0 s relaxation delay. A 2 Hz line broadening was applied. A total of 16 scans was collected. ^{19}F resonances at -41.43 ppm (singlet; TFM peptide) and -75.74 ppm (singlet; trifluoroacetate salt of the TFM-peptide) were observed. A solution of M121TFM Az (2 mg) in 33 mM NH$_4$OAc (pH 5.1; 33% D$_2$O, total volume of 500 μL) was utilized with a 22 522 Hz sweep width, 1.45 s acquisition time, and a 1.0 s relaxation delay. A 2 Hz line broadening was applied. A total of 33 664 scans were collected. The ^{19}F resonance for the M121TFM Az was observed at -39.31 ppm (broad singlet) with a minor resonance at -39.43 ppm. A solution of M121DFM Az (0.2 mg) in 25 mM NH$_4$OAc (pH 5.1; 50% D$_2$O, total volume of 400 μL) was utilized with a 22 522 Hz sweep width, 1.45 s acquisition time, and a 1.0 s relaxation delay under ^{1}H-decoupling conditions. A 2 Hz line broadening was applied. A total of 103 768 scans were collected. The ^{1}H-decoupled ^{19}F spectrum for the M121DFM Az contained resonances centered at approximately -85.60 ppm (broad doublet) and -88.15 ppm (broad doublet) as well as resonances at -93.41 ppm (broad singlet) and a minor resonance at -93.65 ppm (sharp singlet).

Calculation of Log P. The hydrophobicity of the methionine analogue side chains was quantified using the log of the partition coefficient (log P) between octanol and water. Estimation of log P was accomplished using the fragment addition strategy employed by

Leo.[58−60] Briefly, this method calculates a total log P value from the fundamental fragments composing the whole molecule. The fundamental fragment values have been obtained by comparing octanol—water partition experiments on numerous compounds. Additional corrections for bond factors, polar proximity effects, and chain branching have also been determined. These fundamental fragments have been compiled in the CLOGP database developed by the Pomona Medicinal Chemistry Project and are accessible on the web via a simple graphical user interface. The fundamental fragments summed for each side chain examined in this study and any corrective interactions (such as chain extension and proximity effects) are listed individually along with a final calculated value for log P (CLogP) in the tables at the end of the Supporting Information. The selenoether and NH$_3^+$ were assigned fragment constants of -0.59[48] and -3.40,[58] respectively. The log P of ionizable side chains (Lys, Glu, Asp, and His) was determined by pH dependent treatment based on the pK_a of the side chain as previously described.[58] (see Supporting Information table S2). For ionizable side chains, we used the pK_a value reported for that side chain in its type 1 axial mutant protein to calculate the pH dependent log P. This treatment should account for effects that the local protein environment has on the pK_a and thus log P of ionizable residues. Log P values calculated for the side chain of the various axial ligand variants are reported in Supporting Information, Table S1.

Results

Preparation of Azurin Variants Containing Unnatural Amino Acids Using Expressed Protein Ligation (EPL). Previously we reported preparation of Az derivatives in which the conserved axial ligand, M121, was replaced with unnatural amino acids selenomethionine (called M121SeM Az) and norleucine (called M121Nle Az) using EPL (Figure 1).[48] The same protocol was used to obtain Az derivatives in which M121 was replaced with difluoromethionine (called M121DFM Az) or oxomethionine (called M121OxM Az), with similar yields of $\sim$0.2 mg of pure protein per 4 L *E. coli* culture. To increase the yield even further, a modified protocol was employed in preparation of the Az derivative in which M121 was replaced with trifluoromethionine (called M121TFM Az), resulting in $\sim$9 mg of pure protein per 4 L *E. coli* culture. This dramatic $\sim$45-fold increase in yield is attributable to the avoidance of denaturants in the ligation, allowing isolation of more properly folded proteins.

Spectroscopic Characterization. The UV—visible spectra of the five Az derivatives containing unnatural amino acids at the 121 position are very similar to that of wild type Az (Wt Az) (Figure 2), with a strong LMCT band from Cys112 to Cu-(II) being the dominant feature. The OxM and DFM variants display an elevated baseline at shorter wavelengths, which is most likely due to the presence of denatured protein which does not bind copper, as observed in the ^{19}F NMR (vida infra) of DFM Az. The ligand series causes a slight shift in λ_{max} to longer wavelengths, in the order of OxM, Met, SeM, DFM, TFM, Nle, and a total of 6 nm shift overall for all six proteins (Table 1).

The X-band EPR spectra of the variants are also similar to that of Wt Az with some minor differences in g_z and copper hyperfine splittings (Figure 3). Simulation[56,57] of these spectra provided the values reported in Table 1. Similar to the λ_{max} shifts in the UV—vis spectra, the $A_\parallel$ changes are small among the Az derivatives (8 G total). On the other hand, the order of $A_\parallel$ is

(55) Jeuken, L. J. C.; Armstrong, F. A. *J. Phys. Chem. B* **2001**, *105*, 5271−5282.
(56) Nilges, M. J. *Ph.D. Thesis*, University of Illinois **1979**.
(57) Chang, H. R.; Diril, H.; Nilges, M. J.; Zhang, X.; Potenza, J. A.; Schugar, H. J.; Hendrickson, D. N.; Isied, S. S. *J. Am. Chem. Soc.* **1988**, *110*, 625−627.
(58) Abraham, D. J.; Leo, A. J. *Proteins: Struct. Funct. Genet.* **1987**, *2*, 130−152.
(59) Leo, A. J. *Chem. Rev. (Washington, DC)* **1993**, *93*, 1281−1306.
(60) CLOGP Calculation of hydrophobicity as Log P(o/w). http://www.day-light.com/daycgi/clogp (02/22/05).
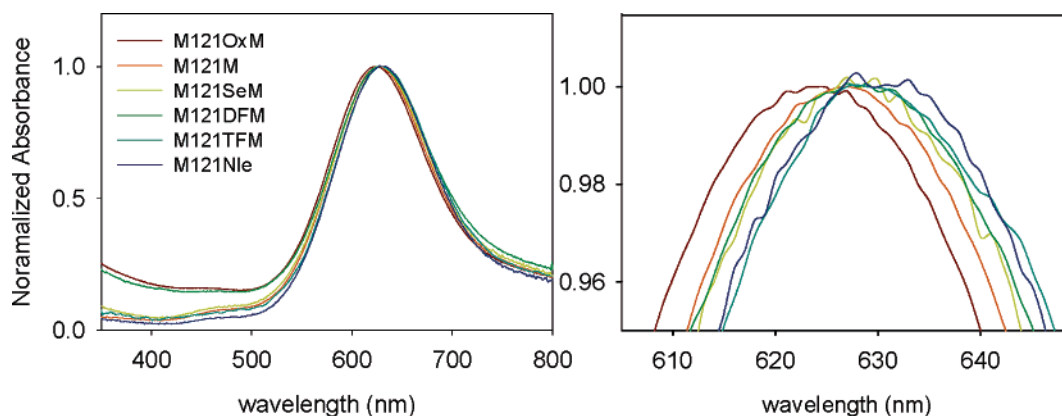
Figure 2. Overlay of the UV−visible absorption spectra of the isostructural axial M121X variant series in Az. The absorbance spectra have been normalized to 1 for convenient comparison.

Table 1. Tabulated Spectroscopic Data and Reduction Potentials for the Isostructural M121X Series

	λ_{max}, nm	EPR g (A)	$E°$ (mV vs NHE)
Wt Az	627	$g_1 = 2.2620$ (63.5 G)	341 ± 3
		$g_2 = 2.0568$ (12.7 G)	
		$g_3 = 2.0388$ (12.7 G)	
M121Nle Az	630	$g_1 = 2.2680$ (58.8 G)	449 ± 3
		$g_2 = 2.0584$ (19.6 G)	
		$g_3 = 2.0402$ (13.4 G)	
M121SeM Az	628	$g_1 = 2.2585$ (60.6 G)	348 ± 4
		$g_2 = 2.0565$ (12.1 G)	
		$g_3 = 2.0383$ (13.2 G)	
M121DFM Az	628	$g_1 = 2.2530$ (56.8 G)	329 ± 5
		$g_2 = 2.0583$ (2.0 G)	
		$g_3 = 2.0274$ (1.9 G)	
M121TFM Az	629	$g_1 = 2.2530$ (56.8 G)	$379 (4$
		$g_2 = 2.0583$ (1.8 G)	
		$g_3 = 2.0295$ (1.9 G)	
M121OxM Az	624	$g_1 = 2.2629$ (55.7 G)	222 ± 5
		$g_2 = 2.0576$ (2.5 G)	
		$g_3 = 2.0305$ (0.8 G)	

different from λ_{max} in the UV−vis. In order of increasing $A_\parallel$, the series is OxM (56 G), DFM (57 G), TFM (58 G), Nle (59 G), SeM (61 G), and Met (64 G).

The ^{19}F resonance for the M121TFM Az is observed at −39.31 ppm in the ^{19}F NMR (Figure 4A). This resonance is broadened in comparison to that of the ^{19}F resonance in the TFM-peptide (−41.43 ppm) before ligation to the N-terminal portion of Az (Figure 4B). In the case of the more complex AB NMR system (proton coupled) found with the DFM nucleus,
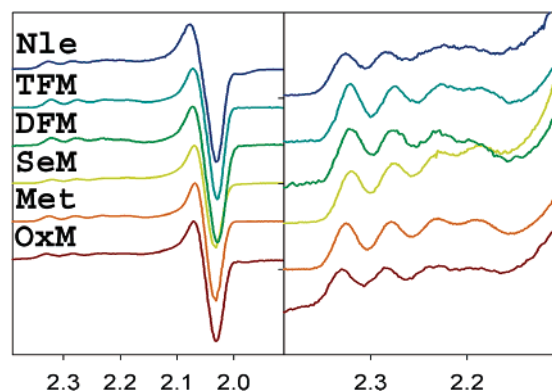

Figure 3. X-band EPR spectra of the isostructural axial M121X variant series in Az. Spectra are stacked in ascending order of M121OxM Az, Wt Az, M121SeM Az, M121DFM Az, M121TFM Az, M121Nle Az. Left, entire scan range. Right, an enlarged g_z region showing the $A_\parallel$ splittings.
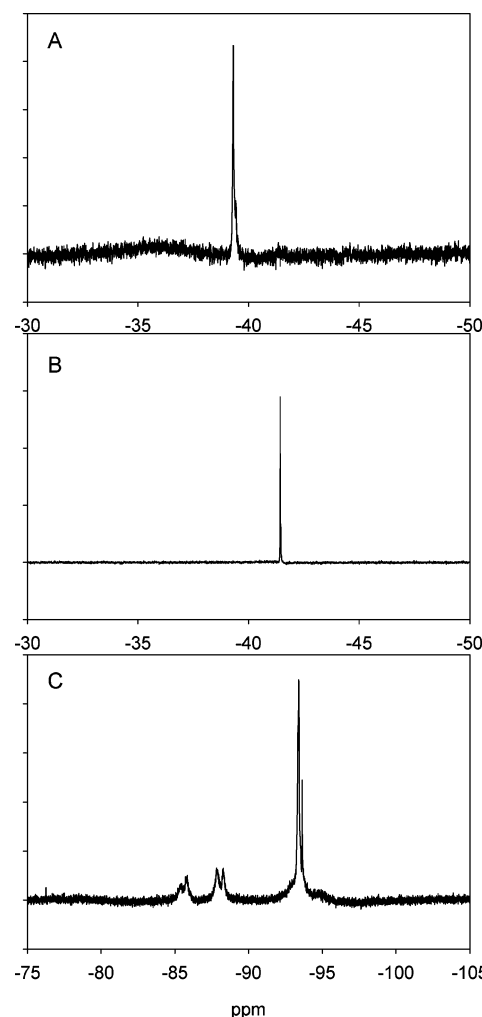
Figure 4. ^{19}F NMR spectra of fluorine-containing axial M121X variant series in Az. (A) M121TFM Az, (B) TFM containing 19-mer peptide, (C) M121DFM Az (^{1}H-decoupled).

a complex ^{19}F resonance pattern resembling two quartets can be observed in the limiting case wherein the DFM side chain is closely packed in a protein core and is unable to exhibit unencumbered conformational movement.[52] This is due to the fact that the two fluorine atoms are diastereotopic; hence, their chemical shifts are nonequivalent, resulting in coupling between the two fluorines as well as proton coupling to each fluorine atom. The chemical shift nonequivalence between the two
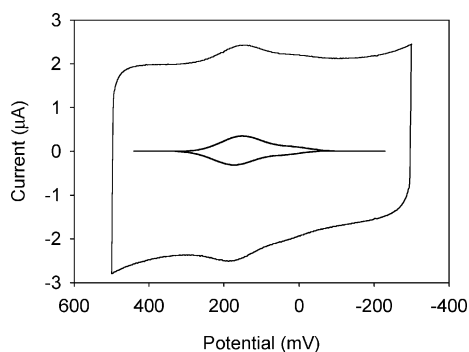
Figure 5. A representative cyclic voltammogram of the M121TFM Az. The nonfaradaic current baseline corrected trace is also shown. Potential is mV vs SCE.

fluorine atoms in the DFM side chain is enhanced if side chain rotation is restricted. Due to the more complex resonance pattern expected for M121DFM Az and the small quantities of M121DFM Az remaining at the end of the biophysical studies for ^{19}F NMR spectroscopic studies, proton-decoupled ^{19}F NMR was undertaken. This technique simplified the ^{19}F resonance pattern for the DFM residue in the labeled Az into two sets of doublets centered at −85.60 ppm (broad doublet) and −88.15 ppm (broad doublet) (Figure 4C), which is indicative of restricted conformational mobility in the protein. The spectrum also contained additional resonances at −93.41 ppm (broad singlet) and −93.65 ppm (minor component) which were most likely produced by proteins containing freely rotating DFM residues due to the presence of completely unfolded M121DFM Az. On the basis of integration of the 19F NMR spectrum, the copper incorporated DFM Az contributes at least 35% of the protein mixture and is responsible for the observed electrochemical and EPR and UV−visible spectroscopic properties.

Electrochemical Measurements. Reduction potentials of the Az derivatives were determined by cyclic voltammetry. The protein was adsorbed onto a pyrolytic graphite edge (PGE) electrode in 20 mM NaOAc, pH 4.0, using a protocol described previously,[55] except that the salt concentration was decreased from 2 M to 100 mM. This was necessary, as some of the variants display multiple peaks at higher salt conditions which we attributed to denaturation of the protein. A characteristic cyclic voltammogram is shown for M121TFM Az (Figure 5). The shoulder observed near 50 mV vs SCE is also present in the buffer scan of a freshly polished electrode and is therefore not generated by the protein sample. The reduction potential observed for Wt Az (341 ± 3 mV vs NHE, see Table 1) is similar to those previously reported under similar conditions.[55] In contrast to the small shifts in λ_{max} and $A_{||}$, the axial ligands have much larger effects on the reduction potentials, spanning 227 mV from M121OxM Az (222 ± 5 mV vs NHE) to M121Nle Az (449 ± 3 mV vs NHE). Reduction potentials of both M121OxM Az and M121DFM Az (329 ± 5 mV vs NHE) are lower than Wt Az, while M121Nle Az is 108 mV higher. M121SeM Az (348 ± 4 mV vs NHE) and M121TFM Az (379 ± 4 mV vs NHE) display potentials intermediate to Wt Az and M121Nle Az.

Discussion

Probing the Precise Role of the Axial Methionine Using Unnatural Amino Acid Analogues. The axial methionine in the type 1 copper sites has been investigated extensively by site-directed mutagenesis.[14−33] However, since none of the natural amino acids is isostructural with methionine, the precise role of this residue in modulating functional properties of the blue copper center still lacks a definitive explanation. Introduction of unnatural amino acid methionine analogues into the copper binding site of Az could help distinguish between different effects such as those created by the electronics of the axial ligand and the steric interactions of this ligand with the copper binding pocket. It should be noted that, although the methionine analogues used in this study were chosen for their close structural similarity to methionine (Figure 1), they are not exact structural replicas. For example, the atomic radius of fluorine and hydrogen are different and the introduction of a methylene unit in Nle in place of sulfur will have some steric differences. Nevertheless, these changes are very close structural analogues of methionine and these structural perturbations should be minor compared to those imposed by conventional mutagenesis.

The DFM and TFM used in this study have been successfully incorporated into a number of other proteins including bacteriophage lambda lysozyme,[52,61,62] bacterial leucine-isoleucine-valine binding protein,[63] calmodulin,[64] green fluorescent protein,[65] and the alkaline protease from *Pseudomonas aeruginosa*.[66] The introduction of a fluorine atom adjacent to the sulfur atom of methionine can result in reduction of the electron density at the sulfur nucleus and an overall increase in the hydrophobicity of the amino acid side chain.[51,61,67] However, introduction of a fluorine adjacent to the sulfur does not preclude sulfur interactions with metals as observed with platinum complexes of *cis*-dichloro[1,2-bis(trifluoromethylthio)propane][68] or of DFM/TFM (Vaughan and Honek, unpublished results).

Spectroscopic Characterizations of Azurin Variants Containing Unnatural Amino Acids. The UV−vis and EPR spectra of all the Az variants investigated in this study are very similar to that of Wt Az (see Figures 2, 3, and Table 1), suggesting that isostructural replacement of Met results in minimal structural perturbation of the copper center. Slight shifts of λ_{max} of the S(Cys)−Cu CT band upon mutation of the axial methionine were observed in the order of M121OxM Az (624 nm), Wt Az (627 nm), M121SeM Az (628 nm), M121DFM Az (628 nm), M121TFM Az (629 nm), and M121Nle Az (630 nm). This shift of the λ_{max} appears to follow the electronegativity of the ligating atom in the axial position. Thus, the axial oxygen atom has the strongest electronegativity and has the most blue-shifted λ_{max}. Next is sulfur and then selenium, following the decreased electronegativity of the ligating atom. This series is complemented by the Nle variant, where no axial metal ligation is possible, having the most red-shifted λ_{max}.

The above trend is further supported by the ^{19}F NMR studies of the fluorinated methionine analogues, which are expected to

(61) Duewel, H.; Daub, E.; Robinson, V.; Honek, J. F. *Biochemistry* **1997**, *36*, 3404−3416.
(62) Duewel, H. S.; Daub, E.; Robinson, V.; Honek, J. F. *Biochemistry* **2001**, *40*, 13167−13176.
(63) Salopek-Sondi, B.; Vaughan, M. D.; Skeels, M. C.; Honek, J. F.; Luck, L. A. *J. Biomol. Struct. Dyn.* **2003**, *21*, 235−246.
(64) McIntyre, D. D.; Tao, Y.; Luykx, A.; Vogel, H. J. *Prog. Biophys. Mol. Biol.* **1996**, *65*, Supplement 1, 33.
(65) Budisa, N.; Pipitone, O.; Siwanowicz, I.; Rubini, M.; Pal, P. P.; Holak, T. A.; Gelmi, M. L. *Chem. Biodiversity* **2004**, *1*, 1465−1475.
(66) Walasek, P.; Honek, J. F. *BMC Biochemistry* **2005**, *6*, 21.
(67) O'Hagan, D.; Rzepa, H. S. *Chem. Commun. (Cambridge, UK)* **1997**, 645−652.
(68) Manojlovic-Muir, L.; Muir, K. W.; Solomun, T. *Inorg. Chim. Acta* **1977**, *22*, 69−74.

display decreased electron density on the methionine sulfur and thus decreased interaction with the copper atom. The shielding of the fluorine atoms may be used to draw inferences about the electron density on the neighboring sulfur atom and thus give a rough indication of the strength of interaction that sulfur may have with the copper ion. The holo M121MTFM Az displays a chemical shift (−39.4 ppm) almost identical to those reported for this methionine analogue in multiple nonmetal binding environments in bacteriophage λ lysozyme (−39.3 to −40.1 ppm).[61,62] However, the holo M121DFM Az ^{19}F chemical shift (−85.6 and −88.2 ppm) is significantly deshielded compared to DFM shifts in the bacteriophage λ lysozyme (−91.2 to −95.5 ppm).[52] Since the ^{19}F NMR chemical shifts of DFM and TFM have been shown to be environmentally sensitive, we infer that the DFM analogue is interacting more strongly with the copper ion than its trifluoro cousin, although TFM is somewhat less sensitive to environmental factors than DFM. Furthermore, the S(TFM)−Cu interaction in the M121TFM Az is very weak with no discernible perturbation of the fluorine chemical shift. These observations clearly establish the axial ligand strength of the fluoromethionine analogues somewhere between Wt Az and M121Nle Az, with the relative assignment of M121DFM Az possessing a stronger axial ligand than M121TFM Az. The observation of UV−visible λ_{max} values for the fluoromethionine analogues, which are intermediate to Wt Az and M121Nle Az, supports the correlation of axial ligand strength with shifting λ_{max}.

The EPR data for the M121X Az series plotted in Figure 3 and summarized in Table 1 do not follow the trend of increasing electronegativity of the axial ligand. The $A_{\parallel}$ value in the EPR is a measure of the amount of interaction between the unpaired d^9 copper electron and the copper nucleus. Increased hyperfine splitting may therefore be indicative of greater electron density on the copper atom and reduced delocalization onto the copper ligands.[5] For our series, M121OxM Az displays the smallest hyperfine splitting. However, all other variants also display smaller hyperfines than Wt Az. The very small spectroscopic changes and apparent lack of definitive trends across these different spectroscopic techniques demonstrate the weak nature of the axial ligand interactions and indicate that the role of the axial ligand is not to alter the electronic structure significantly through bonding to the type 1 copper site.

Correlations between Reduction Potentials and Properties of the Axial Ligands. In contrast to the minor changes observed by UV−vis and EPR spectroscopic techniques, large variations in reduction potential were observed for this series. As reported in Table 1, the reduction potential increased for M121SeM Az (348 mV vs NHE, Δ +7 mV), M121TFM Az (379 mV vs NHE, Δ +38 mV), and M121Nle Az (449 mV vs NHE, Δ +108 mV), while the potential decreased for M121DFM Az (329 mV vs NHE, Δ −12 mV) and M121OxM Az (222 mV vs NHE, Δ −119 mV). Previous NMR experiments have suggested that the strength of the axial ligand interaction may not be directly correlated to the covalency of the Cu-Cys bond.[69,70] The nonbonded effects of the axial ligand, such as hydrophobicity, on the reduction potential of the type 1 copper site have
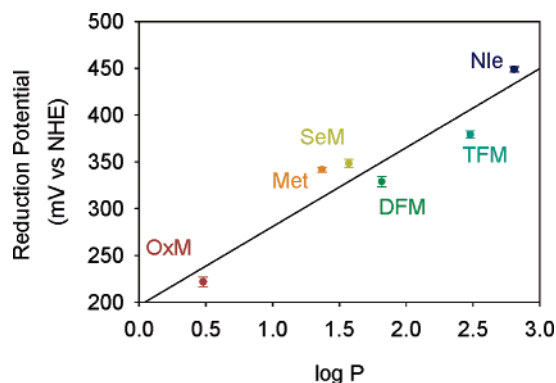

Figure 6. Plot of reduction potential vs log *P* for the isostructural methionine variants. The black line is a linear regression with an r^2 value of 0.92.

previously been proposed to play an important and even defining role.[15,48] In order to examine the existence of such a correlation, the hydrophobicities, quantified as the log of the partition coefficient (log P) between octanol and water, of each side chain in our series were calculated following the method of Leo.[58-60] A plot of reduction potential vs log *P* of each type 1 copper variant reveals a linear correlation with an r^2 factor of 0.922 (Figure 6). The wide range of reduction potentials in this series encompasses nearly the entire range of reduction potentials reported for the Az type 1 site.[15] Due to the isostructural nature of the mutations, large structural changes resulting in increased solvent exposure of the copper ion are not expected to be the source of these perturbations. The strong linear correlation over such a large range with very minimal perturbation in the spectroscopy and structure of the axial ligand indicate that hydrophobicity is the dominant effect in axial ligand tuning of the reduction potential.

The pronounced correlation of reduction potential to hydrophobicity in our isostructural series raises the question of the generality of this trend in all type 1 copper sites. From the literature, we were able to compile an extensive list of type 1 copper proteins wherein the axial ligand had been mutated and the reduction potential determined. Average reduction potentials for Az,[15,19,46,48,71,72] nitrite reductase,[24,25] amicyanin,[26] rusticyanin,[27] psuedoazurin,[28] laccase,[29] stellacyanin,[30,31] mavicyanin,[32] and umecyanin[33] are compiled in Supporting Information Table S1 where they have been grouped according to the nature of the native axial ligand. Since our isostructural methionine replacement series predicted the existence of a correlation between reduction potential and hydrophobicity by means of a comparison of log *P* and E^o, we examined several type 1 sites in this fashion. Figure 7 shows a plot of the reduction potential vs log *P* of the axial ligand. For ionizable side chains we used the pK_a value reported for that side chain in its type 1 axial mutant protein to calculate the pH dependent log *P* (see Supporting Information). This treatment should account for effects that the local protein environment has on the pK_a and thus log *P* of ionizable residues.

For clarity, we have plotted only proteins for which three or more axial ligands in the same protein have been reported. Overall, no correlation is evident. However, strong linear

(69) Donaire, A.; Jiménez, B.; Fernández, C. O.; Pierattelli, R.; Niizeki, T.; Moratal, J.-M.; Hall, J. F.; Kohzuma, T.; Hasnain, S. S.; Vila, A. J. *J. Am. Chem. Soc.* **2002**, *124*, 13698−13708.
(70) Fernández, C. O.; Niizeki, T.; Kohzuma, T.; Vila, A. J. *J. Biol. Inorg. Chem.* **2003**, *8*, 75−82.

(71) Chi, Q. J.; Zhang, J. D.; Andersen, J. E. T.; Ulstrup, J. *J. Phys. Chem. B* **2001**, *105*, 4669−4679.
(72) Fujita, K.; Nakamura, N.; Ohno, H.; Leigh, B. S.; Niki, K.; Gray, H. B.; Richards, J. H. *J. Am. Chem. Soc.* **2004**, *126*, 13954−13961.
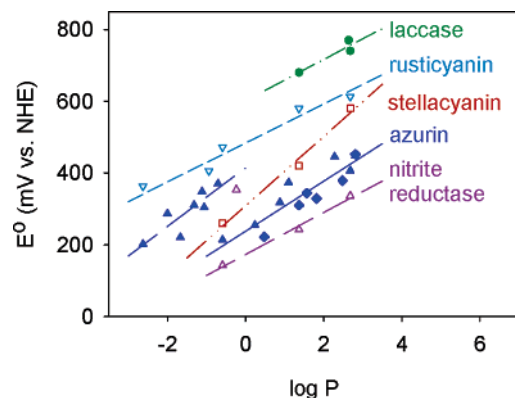
Figure 7. Plot of reduction potential vs log *P* for various axial ligand variants in type 1 copper sites from different proteins. Species are Az (blue filled triangles, isostructural variants diamonds), nitrite reductase (purple hollow triangles), rusticyanin (blue hollow inverted triangles), laccase (green filled circles), and stellacyanin (red hollow boxes). Lines represent least-squares fits to the data for each protein.
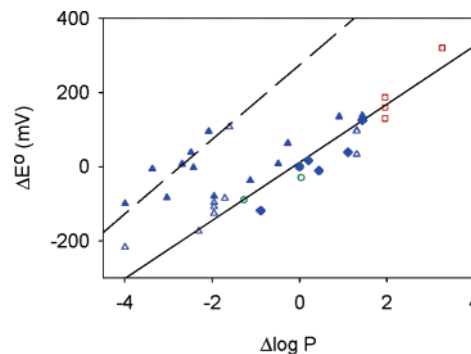

Figure 8. Plot of the change in reduction potential vs change in log *P* relative to wild type for type 1 sites. Native axial ligands are methionine (Az, filled triangles; Az isostructural replacements, diamonds; others hollow triangles), phenylalanine (circles), glutamine (squares). The lines represent least-squares fits to the lower (solid) and higher (dashed) potential variants as grouped by residual analysis using the least-squares fit to the isostructural variants presented in this work.

dependence of the reduction potential on the hydrophobicity of the axial ligand is observed when each protein is considered individually, even though the absolute value of the reduction potential varies for different proteins with the same axial ligand. Surprisingly, in Az, the most hydrophilic substitutions appear to cluster into a separate line about 150 mV above the one predicted by the isostructural substitutions. We note that the nitrite reductase variant Met182Thr also displays a reduction potential that does not correlate linearly with other variants reported for this protein but which appears to correlate with the Az high potential line. Observation of the high potential variants in two different type 1 copper proteins suggests that this effect is not unique to Az but instead corresponds to a fundamental property of the type 1 site (vida infra).

It appears from the plot in Figure 7 that there are factors within each protein which set a base reduction potential, and the axial ligand is able to tune the reduction potential linearly above this base. Computational studies have predicted that the axial ligand is not the major determinant of the relative reduction potentials in type 1 sites from different proteins,[8] and our findings here are in harmony with this conclusion. Additionally, it is important to note that similar slopes for nitrite reductase (49), rusticyanin (51), and laccase (58) indicate that altering the hydrophobicity of the axial ligand has effects of nearly the same magnitude in these proteins. Stellacyanin and Az, with a slope of 98 and 70 (lower potential line), respectively, appear to be more sensitive to changes in the hydrophobicity of the axial ligand than the other type 1 sites; however, the correlation to hydrophobicity in these proteins is still strongly linear. This stronger dependence on the hydrophobicity may be influenced by the greater active site solvent exposure of stellacyanin[30] and the axial carbonyl ligand in Az, both of which will serve to make the overall copper binding site more polar and thus more sensitive to the hydrophobic nature of the axial ligand.

It should be noted that due to differing experimental conditions (pH, ionic strength, measurement technique) utilized by researchers, the variation in measurements of reduction potential for a given variant may be substantial, and reduction potentials ranging over 65 mV have been reported for the same wild type azurin (Supporting Information, Table S1). Variations of similar magnitudes have been observed over the pH range from 4 to 8 for both wild type Az and M121L Az.[15] As these pH conditions

represent extremes, the observed difference in reduction potential of about 50 mV gives an estimation of the maximum amount of change inducible by different experimental conditions and which is small when compared to the full range of reduction potential changes observed (>200 mV). We note specifically that the isostructural Met variants of azurin (Figure 7, diamonds) have a slope that is steeper than that obtained using all of the axial Az variants on the lower line (Figure 7, triangles). Since the least-squares fit is higher for the isostructural variants (0.92) than for all lower line Az variants (0.84), we interpret this observed difference to different experimental conditions utilized to obtain the various data points. While caution must be exercised in comparing data obtained under such differing conditions, the overall linear dependence is quite clear for all of the proteins examined and demonstrates the dominating effect that the hydrophobicity of the axial ligand has on the reduction potential. The diverse nature of conditions utilized for data collection, coupled with the small number of data points available for many of the proteins, may mean that the small observed differences in slope are insignificant even between the various type 1 copper proteins.

In order to eliminate effects from the different protein environments, measurement techniques, and experimental conditions, thus evaluating only the effect of the change in the axial ligand, we determined the change in reduction potential (ΔE^o) and log *P* (Δlog *P*) by subtracting the values for the native axial ligand for each individual report of a mutation. These values were then averaged for all reports of a given axial variant for each protein (Supporting Information, Table S1). Upon initial inspection, the resulting plot of ΔE^o vs Δlog *P* displays a high degree of scatter and low linear correlation. However, further examination of the error residuals using the least-squares fit of the isostructural data reported in this paper (Figure S1) revealed that there are two sets of reduction potentials represented in this data (Figure 8), one of which differs greatly from the line predicted by the isostructural data, and both of which display strong linear correlations. Treatment of the data from each set independently yields two nearly parallel lines (high potential line, slope $=100$, $r^2 = 0.82$, dashed, and low potential line, slope $= 78$, $r^2 = 0.87$, solid) (Figure 8). It should be noted that this effect may not be attributed solely to the strength of the axial ligand. Gly, Asn, and Thr, all of which should display no metal coordination, are on the high potential line, and stronger
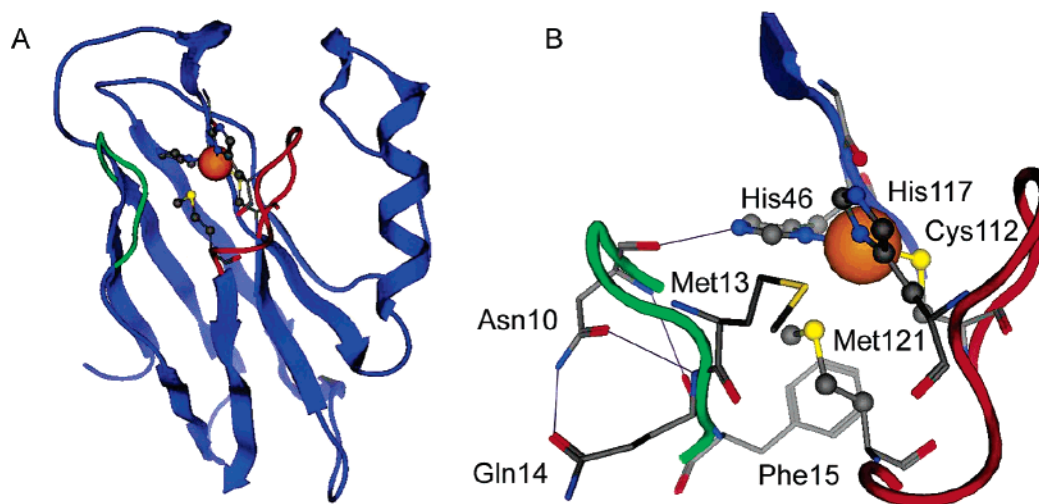
Figure 9. Ribbon diagram of Az (PDB ID No. 4AZU[78]) showing the hydrophobic (green) and ligand (red) loops of the type 1 site. Copper atom is space-filling, copper ligands are ball and stick, and all other residues are stick. (A) The overall protein topology. (B) Vicinity of the copper binding site showing the hydrophobic clamp around Met121 generated by Met13 and Phe15. Hydrogen bonds (thin purple lines) that are maybe disturbed by mutation of the axial ligand are also shown.

ligands Gln and His (pH 7.0) are on the lower line. Coordination of oxygen is also an insufficient explanation, as Thr, which is too short to coordinate, is on the upper line while Gln and OxM which do coordinate are on the lower line. Finally, the location of Gln on the lower line and Asn on the upper line indicates that factors other than the nature of the coordinating oxygen atom are important. The similarity in slopes between both high and low potential lines and the isostructural line (slope = 84) is indicative of the continued effect of decreasing the hydrophobicity of the axial ligand while the large (~150 mV) jump in reduction potential between the two lines must be a manifestation of another secondary effect of altering the axial ligand.

The primary effect expected upon decreasing the hydrophobicity of the axial ligand is the preferential stabilization of the Cu^{2+} relative to the Cu^+ oxidation state. This should result in a lowering of the reduction potential. It has been proposed previously that disruption of the hydrogen-bonding network in type 1 copper sites can lead to higher reduction potentials due to the relative stabilization of the Cu^+ oxidation state.[74,75] These observations are attributed to decreased stability of the protein fold allowing for less ligand constraint of the reduced copper ion.

In Az, the axial ligand does not participate in hydrogen bonding but is involved in hydrophobic interactions with the residues of loop 10–15 (hereafter, the hydrophobic loop, shown in green in Figure 9a), which is next to the copper binding site. In particular, Met13 and Phe15 form a conserved hydrophobic C clamp around the axial ligand Met121 (Figure 9b). These types of hydrophobic interactions are expected to be the force dominating the fold in this part of the protein since there are almost no interloop hydrogen bonds on this side of the metal

binding site.[74] Alterations to the hydrophobic nature of the axial ligand are thus predicted to directly influence the stability of the protein fold. In the case of the Met121Ala variant, the stability of the apo protein is less than apo wild type[76,77] as expected if an important stabilizing interaction is removed. Among potential explanations, perturbation of the protein fold induced by the loss of hydrophobic interactions and/or the disruption of hydrogen bonds may be contributing factors for the large jump in reduction potential for very hydrophilic axial variants. Support of these hypotheses should come from studies of the relative stabilities of the Az axial ligand variants, and such experiments are underway.

Conclusions

Isostructural replacement of the axial ligand from the type 1 copper site in the electron-transfer protein azurin has allowed the observation of a linear correlation between the hydrophobicity of the axial ligand and the reduction potential of the copper ion. Extension of this type of analysis to other type 1 copper-containing proteins indicates a strong linear correlation between change in hydrophobicity and change in reduction potential, independent of the protein scaffold (Figure 8). This led to the conclusion that the different slopes of the individual proteins observed in Figure 7 arise from minor differences, and the effect of the axial ligand is nearly uniform for all type 1 centers. Given the wide range of reduction potentials, protein scaffold types, experimental conditions, measurement techniques, and steric modifications represented in this sample set, the appearance of any correlation is unexpected and argues strongly that the dominant effect of the axial ligand in tuning the copper reduction potential is through hydrophobic interactions. These observations were only possible because of the isostructural axial ligand replacements afforded by unnatural amino acids and demonstrate the utility of express protein ligation in the study of metallo-

(73) Karlsson, B. G.; Tsai, L.-C.; Nar, H.; Sanders-Loehr, J.; Bonander, N.; Langer, V.; Sjölin, L. *Biochemistry* **1997**, *36*, 4089−4095.
(74) Machczynski, M. C.; Gray, H. B.; Richards, J. H. *J. Inorg. Biochem.* **2002**, *88*, 375−380.
(75) Wittung-Stafshede, P.; Gomez, E.; Ohman, A.; Aasa, R.; Villahermosa, R. M.; Leckner, J.; Karlsson, B. G.; Sanders, D.; Fee, J. A.; Winkler, J. R.; Malmström, B. G.; Gray, H. B.; Hill, M. G. *Biochim. Biophys. Acta* **1998**, *1388*, 437−443.
(76) Marks, J.; Pozdnyakova, I.; Guidry, J.; Wittung-Stafshede, P. *J. Biol. Inorg. Chem.* **2004**, *9*, 281−288.
(77) Pozdnyakova, I.; Guidry, J.; Wittung-Stafshede, P. *Biophys. J.* **2002**, *82*, 2645−2651.
(78) Baker, E. N. *J. Mol. Biol.* **1988**, *203*, 1071−1095.

proteins. On top of the hydrophobicity modulation, the existence of high and low potential states for the type 1 centers has also been revealed from the analysis. Destabilization of the protein fold by disruption of hydrophobic or hydrogen bonding interactions may contribute the 150 mV jump between the two sets of reduction potentials.

Supporting Information Available: Fragment constants used in calculation of log P for each amino acid, pH dependent treatment of log P calculations, and complete table of reduction potentials for type 1 sites from the literature. This material is available free of charge via the Internet at http:// pubs.acs.org.

JA062732I